High-energy gamma ray emission mechanisms

Alina Donea
School of Mathematical Sciences
Monash University

Two gamma-ray instruments:
Large Area Telescope (LAT) 20 MeV - >300 GeV
Gamma-ray Burst Monitor (GBM) 10 keV - 25 MeV
1 eV -> 14.4 Hz

E	Freq	Log10[Freq]
1 eV	2.4 10^{14}	14.4
1 MeV	2.4 10^{20}	20.4
1 GeV	2.4 10^{23}	23.4
300 GeV= 3 10^{11} eV	7.5 10^{25}	25.9
1 TeV	2.4 10^{14}	26.4

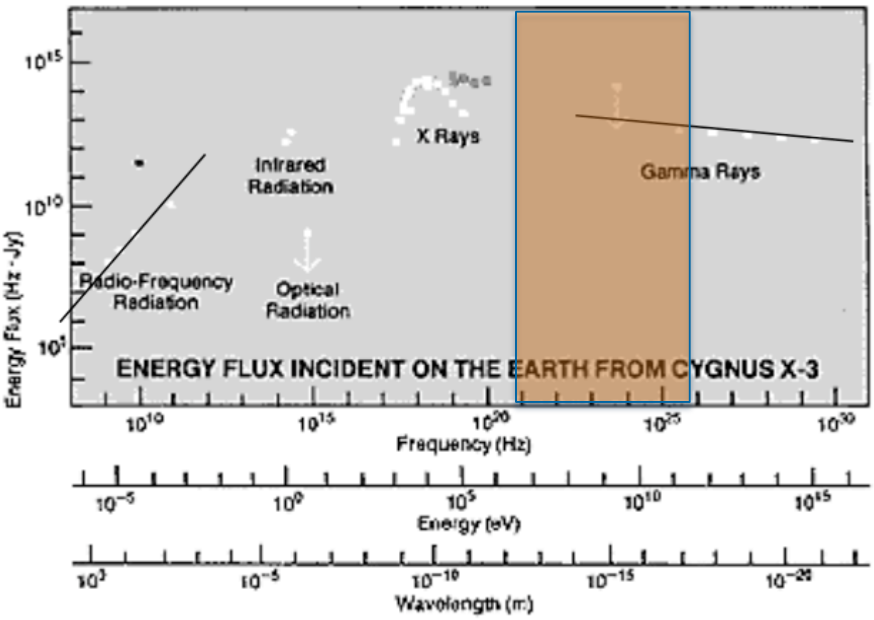

Steps:

- General
- Hadronic vs leptonic model of emission of GeV photons
- Types of emissions
- Particle accelerations (e, CR)
- Examples: synchrotron, IC, bremsstrahlung, pio
- Case studies

•Galactic diffuse emission
SNR
•Pulsars
•Blazars

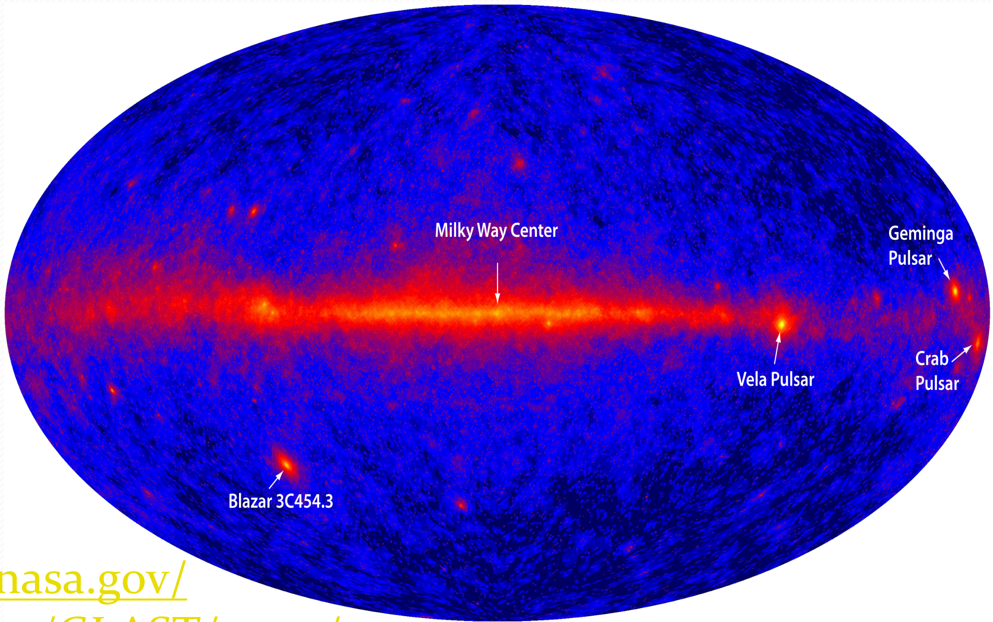

- http://www.nasa.gov/mission_pages/GLAST/news/glast_findings_media.html
- First-Light Sky Map with 95 hrs (4 days)

Aims for an astro person:

- To visualize the source at different wavelength
- To understand its environments
- To model radio to X-ray, and gamma-ray spectra
- Multiwavelength analysis, correlation
- Variability , time dependent models

How much physics do we need to know?

- Electromagnetic theory to understand radiation from fast moving charges and particle acceleration mechanisms.
- • Astrophysical fluid dynamics, including some magnetohydrodynamics (MHD), to understand mass, momentum and energy transport in high energy environments and hydrodynamical acceleration mechanisms.
- • Special and General Relativity to understand the relativistic limits of radiation processes and fluid dynamics.
- **Hadronic versus leptonic gamma-rays**

Hadronic and leptonic models:

- Synchrotron radiation $p, e^- + B \rightarrow p, e^- + \gamma$
- Inverse Compton (IC) $e^- + \gamma \rightarrow e^- + \gamma$

- Proton-proton inelastic collisions $p + p \rightarrow p + p + a\,\pi^0 + b(\pi^+ + \pi^-)$
- Photohadronic interactions ($p\gamma$) $p + \gamma \rightarrow p + e^+ + e^-$

$$e^\pm + B \rightarrow e^\pm + \gamma$$

$$p + \gamma \rightarrow p + a\pi^o + b(\pi^+ + \pi^-) \qquad \pi^o \rightarrow 2\gamma$$

$$p + \gamma \rightarrow n + \pi^+ + a\pi^o + b(\pi^+ + \pi^-) \qquad \pi^\pm \rightarrow \mu^\pm + \nu_\mu(\bar{\nu}_\mu) \qquad \mu^\pm \rightarrow e^\pm + \nu_e(\bar{\nu}_e) + \bar{\nu}_\mu(\nu_\mu)$$

Emission mechanisms of gamma-rays

- T ~ E/k > ~ 10^7 K at which matter is fully ionised, so we are dealing with free particles in *plasma*.

γ - rays are produced in the interstellar medium by interactions of CR protons with:

- He (π^0 –decay)
- Electrons (bremsstrahlung) with gas
- electrons with the interstellar radiation field via inverse-Compton scattering.

Particle acceleration and energy losses

- How does the energy spectrum of synchrotron-emitting electrons evolve? Synchrotron, inverse Compton and adiabatic losses.
- Where must particle acceleration take place?
- Fermi acceleration at strong shocks (SNR)
- Other acceleration mechanisms (winds, flares, etc)

- Adiabatic losses (particles expand and do **p dV** work). Loss rate $\propto$E:

$$-(dE/dt)_{ad} = (\nabla.\mathbf{v})E/3$$

(ultrarelativistic limit)

- Electron energy distribution

$$n(E)\, dE = n_o\, E^{-k}\, dE.$$

How does it evolve with time?

- Synchrotron and inverse Compton losses per electron for isotropic pitch angle distribution:

$$-(dE/dt)_{sync} = (4/3)\sigma_T c\, \gamma^2 u_{mag}$$
$$-(dE/dt)_{iC} = (4/3)\sigma_T c\, \gamma^2 u_{rad}$$

Individual galactic sources

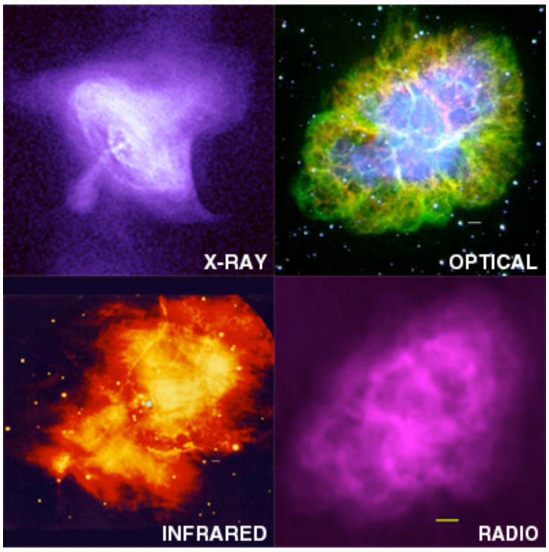

Crab nebula

Cas A

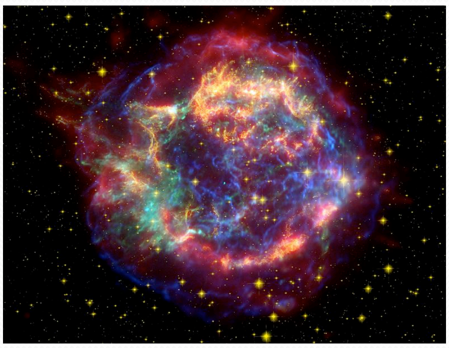

A false color image composited of data from three sources.
Red is infrared data from the Spitzer Space Telescope,
orange is visible data from the Hubble Space Telescope,
and blue and green are data from the Chandra X-ray Observatory

Gamma rays linked to Cosmic Rays Acceleration/Origin

- It is widely believed that Supernova Remnants (SNRs) constitute the major source population in our Galaxy responsible for the observed CRs.
- The main phenomenological argument, formulated by the pioneers of the field, is based on the fact that the power to maintain the galactic population of CRs is estimated to be ≈ 10 per cent of the total mechanical energy released by SN explosions in our Galaxy.
- But other potential source populations like pulsars, X-ray binaries (microquasars), young stars with powerful mechanical winds also meet, at least formally, this energy requirement
- The second key argument in favor of SNRs as sources of galactic CRs has a theoretical background, namely it relies on the theory of diffusive shock acceleration (DSA) applied to young SNRs
- Over the last 20 years the basic properties of this model have been comprehensively studied and cross-checked using different computational approaches.
- The high acceleration efficiency, coupled with hard energy spectra of protons extending well beyond 10 TeV, should lead to VHE γ -ray fluxes of hadronic origin.
- Since the same electrons can also radiate radio and GeV gamma-rays through inverse Compton (IC) scattering, we deal with two competing emission processes responsible (leptonic origin of gamma-ray emission)
- from these SNRs was and remains the favored model of both the gamma-ray and X-ray communities.

Origin of Cosmic-Rays

- Where do protons come ? Cosmic-rays are dominated by protons.
- Photons keep the information of the original source position (complementary to measuring charged particles which are effected by magnetic field)
- We need to detect hadronic interaction, since the emission from leptonic interaction (synchrotron and inverse-Compton) is mainly from electrons.

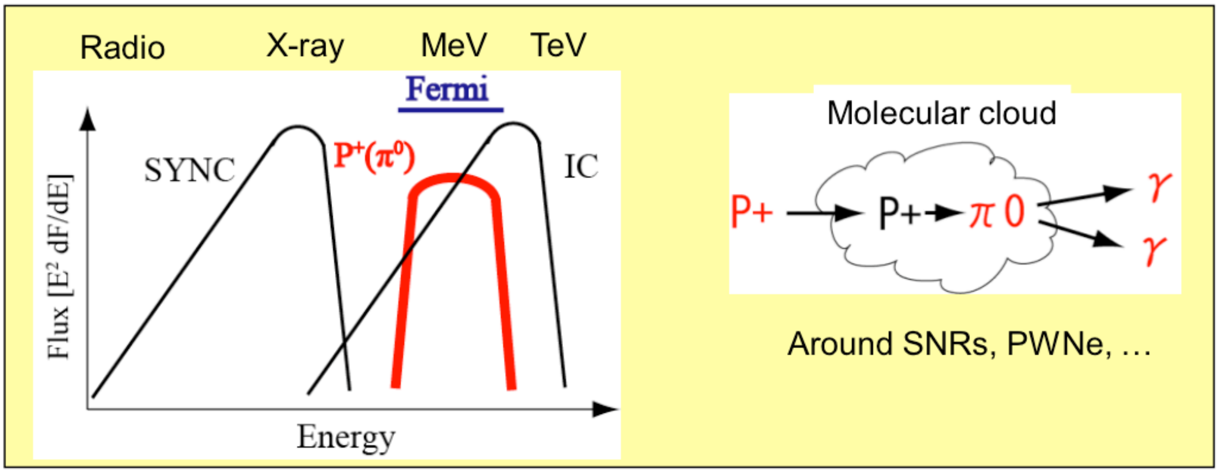

MeV gamma-rays are very important to reveal accelerated protons directly.

Synchrotron radiation

- Synchrotron and inverse Compton losses per electron for isotropic pitch angle distribution:

$$-(dE/dt)_{sync} = (4/3)\sigma_T c\, \gamma^2 u_{mag}$$

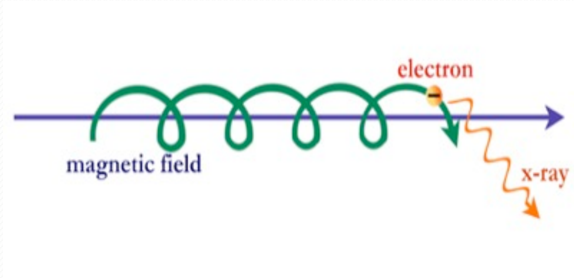

Radiative case study:

Emission of SN 1006 produced by accelerated cosmic rays

E. G. Berezhko - L. T. Ksenofontov - H. J. Völk 2004

- Synchrotron emission flux as a function of frequency for the same two cases as in Fig. 2. Solid and dashed lines correspond to efficient and inefficient proton acceleration, respectively. The observed X-ray (in black color: Hamilton et al. 1986; in red color: Allen et al. 1999) and radio emissions (in black color: Reynolds 1996) are shown.

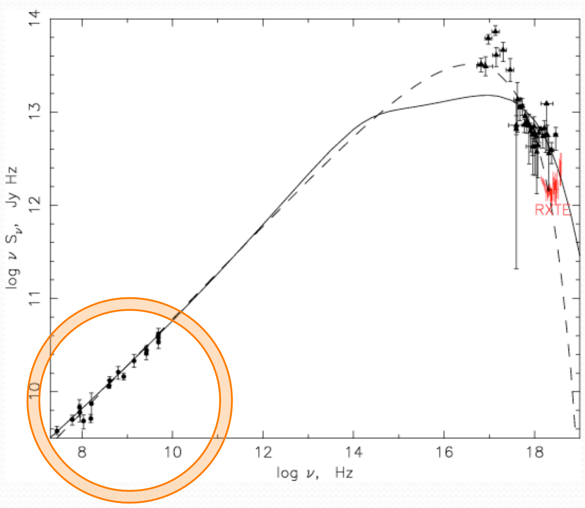

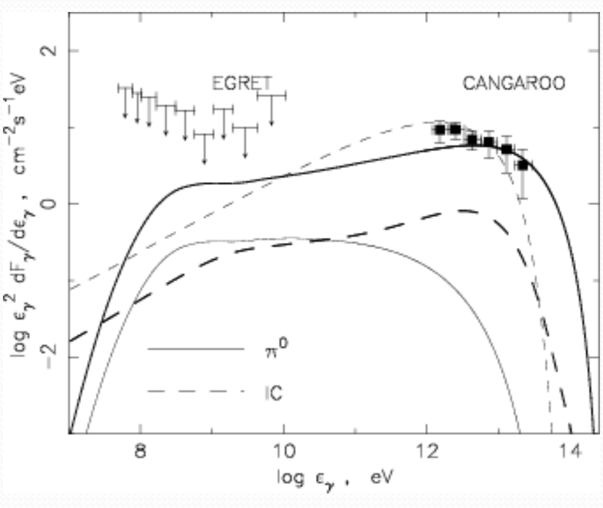

electron bremsstrahlung

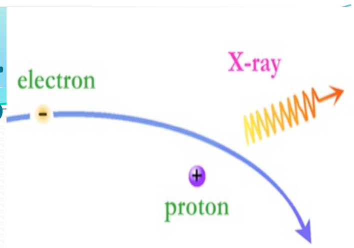

- Bremsstrahlung (free-free) - acceleration of electrons in electrostatic fields of ions and nuclei.
- NonRelativistic:

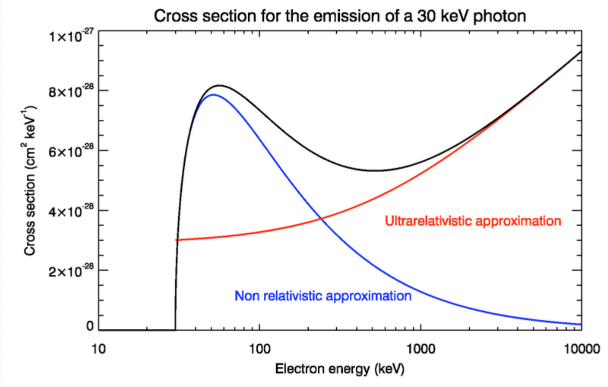

$$\epsilon_{\rm ff} = 1.4 \times 10^{-27} T^{1/2} n_e n_i Z^2 g_B$$

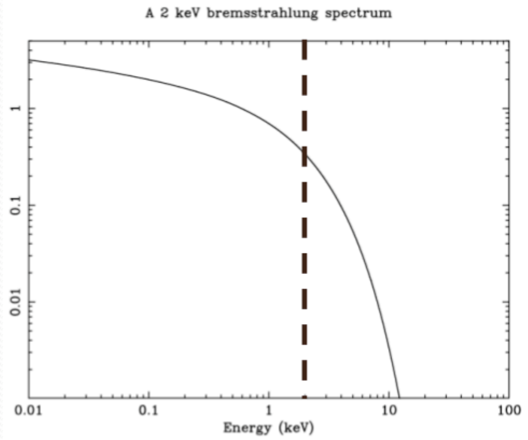

$$P_\nu = 2\pi\, P_\omega = \frac{dE}{dt\, d\nu} = \frac{n_i\, Z^2\, e^6}{6\,\pi^2\, \epsilon_0^3\, c^3\, m_e^2\, v}$$

$$h\nu = 10^5 eV$$

$$T = \frac{h\nu}{k} = 1.2 \times 10^9 K$$

electron bremsstrahlung

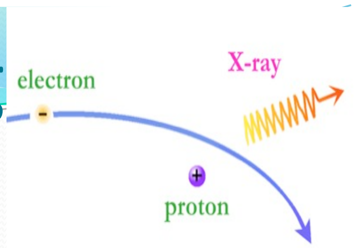

- We want to calculate the emission coefficient for a power-law spectrum of relativistic electrons and finally the electron energy loss rate.

- for relativistic particles: one needs to Lorentz transform the Coulomb field of the scattering particle into the restframe of the particle to be scattered.

It is useful to write the photon energy in units of the electron rest-mass energy, $E = \epsilon\, m_e c^2$, equivalent to the Lorentz factor for the total electron energy. Then with a power-law spectrum of electrons $N(\gamma) = N_0\, \gamma^{-s}$ and $b_{\rm min} = \frac{\gamma \hbar}{mc}$ we derive

$$j_\epsilon = \frac{d\epsilon}{d\epsilon\, dt\, dV\, d\Omega} = \frac{\epsilon}{4\pi} \int d\gamma\; n_i\, \beta c\, N(\gamma)\, \frac{d\sigma}{d\epsilon}$$

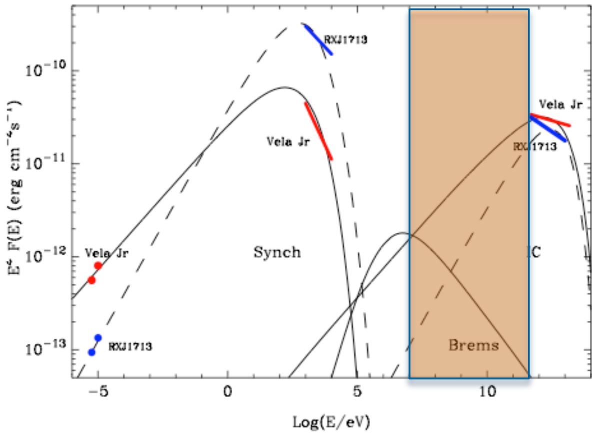

Figure 8: The integrated broad band SEDs of RX J1713.7-3946 and Vela Junior, and their interpretation within the framework of the one-zone leptonic model. The shown power-law presentations of gamma-ray fluxes are from the best fits to the HESS data. Three components of radiation - synchrotron, IC and bremsstrahlung - are shown. The calculations for RX J1713.7-3946 are performed for the following parameters: electrons are accelerated and injected continuously, over the last 1000 yr, into a region with magnetic field 10 μG and gas density $n = 0.1$ cm^{-3}. It is assumed that the electrons are injected with a rate $L_e = 10^{37}(d/1\text{kpc})^2$ erg/s and energy spectrum given by Eq.(1) with $\alpha = 2$ and $E_0 = 50$ TeV. The model parameters used for calculations of the SED of Vela Junior are similar, except for $\alpha = 2.37$, and $L_e = 8 \times 10^{38}(d/1\text{kpc})^2$ erg/s.

Radiative case study:

- The same multi-TeVelectrons responsible for synchrotron X-rays contribute to the TeV γ-ray emission through the inverse Compton scattering.

Aharonian 1999

Radiative case study:

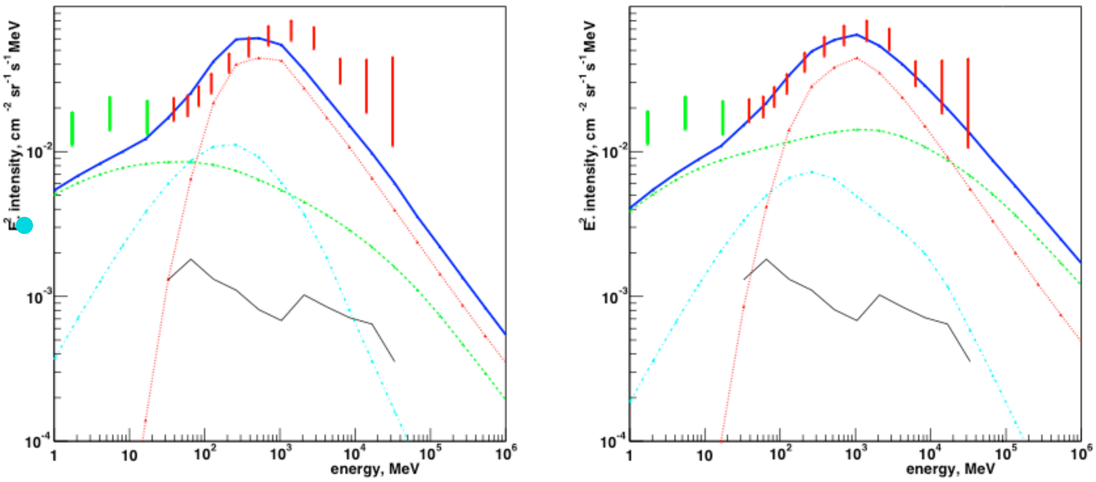

Figure 14: γ-ray spectrum of inner Galaxy ($330° < l < 30°, |b| < 5°$) for model based on the directly-observed CR spectra and modified spectra shown in Fig. 13. Red bars: EGRET data, including points above 10 GeV, see (151). Green bars: COMPTEL. Light blue line: bremsstrahlung, green line: inverse Compton scattering, red line: π^0-decay, black line: extragalactic background, dark blue line: total. This is an update of the spectra shown in (113).

Cosmic-ray propagation and interactions in the Galaxy
Andrew W. Strong , Igor V. Moskalenko, Vladimir S. Ptuskin 2007

Inverse Compton

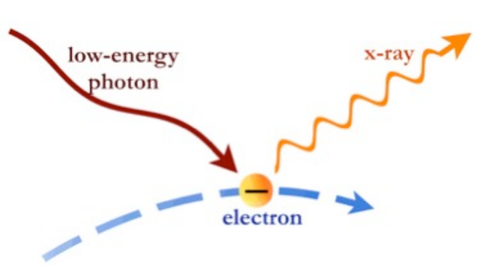

Photon scattering by electrons - Overview

	Low energy photons $\hbar\omega \ll m_e c^2$	**High energy photons** $\hbar\omega \geq m_e c^2$
$v \ll c$	Thomson scattering Classical treatment	Compton scattering Quantum treatment incorporating photon momentum Wavelength change
$v \sim c$	$\gamma\hbar\omega \ll m_e c^2$ Inverse Compton Photons gain energy from relativistic electrons Approximate with classical treatment in electron rest frame	$\gamma\hbar\omega \geq m_e c^2$ Inverse Compton Quantum treatment in electron rest frame Photons gain energy from relativistic electrons

The Klein-Nishina cross section

In addition to the effects of photon momentum, quantum corrections also modify the cross section for Compton scattering. The exact expression for the differential cross section for Compton scattering is derived from quantum electrodynamics and is known as the *Klein-Nishina* formula:

$$\frac{d\sigma_{\rm KN}}{d\Omega} = \frac{1}{2} r_0^2 \frac{\varepsilon_1^2}{\varepsilon^2} \left(\frac{\varepsilon}{\varepsilon_1} + \frac{\varepsilon_1}{\varepsilon} - \sin^2\Theta \right)$$

where $r_0 = e^2/(4\pi\epsilon_0 m_e c) = 2.82 \times 10^{-15}$ m is the classical electron radius (defined in Lec. 8). This reduces to the classical differential Thomson cross section in the limit $\varepsilon_1 \sim \varepsilon$, *viz.* $d\sigma_{\rm T}/d\Omega = \frac{1}{2} r_0^2 (1 + \cos^2\Theta)$. The *total* cross section is obtained by integrating over solid angle, $\sigma_{\rm KN} = 2\pi \int_{-1}^{+1} (d\sigma_{\rm KN}/d\Omega)\, d\cos\Theta$:

$$\sigma_{\rm KN} = \sigma_{\rm T} \frac{3}{4} \left\{ \frac{1+x}{x^3} \left[\frac{2x(1+x)}{1+2x} - \ln(1+2x) \right] + \frac{1}{2x} \ln(1+2x) - \frac{1+3x}{(1+2x)^3} \right\}$$

where $x \equiv h\nu/m_e c^2$.

Kuncic 2008

The overall effect of $\sigma_{\rm KN}$ is to reduce the scattering cross section relative to $\sigma_{\rm T}$ at high photon energies. Thus, *Compton scattering becomes less efficient at high energies.* The decline is shown in the plot below.

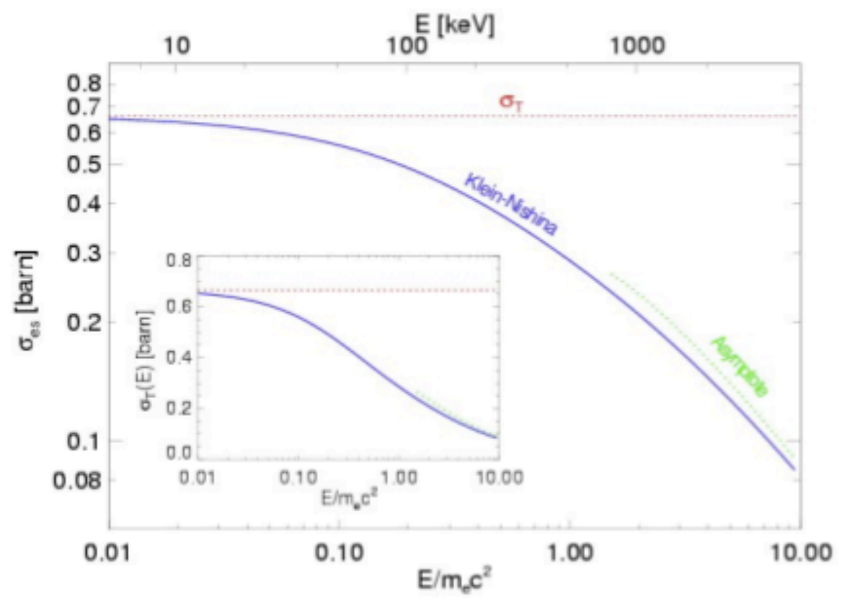

For $x \gg 1$, the asymptotic solution is $\sigma_{\rm KN} \sim \frac{3}{8}\sigma_{\rm T} x^{-1}\left(\ln 2x + \frac{1}{2}\right)$

Kuncic 209

Scattering of blackbody photons

The above derivation implies that if the incident photon distribution is a blackbody spectrum, the resulting spectrum after a single scattering by nonthermal electrons should be a power law. For a blackbody, we have

$$n(\varepsilon) = \frac{8\pi}{(hc)^3}\varepsilon^2\left[\exp\left(\frac{\varepsilon}{kT}\right) - 1\right]^{-1} \tag{22}$$

Emitted power for a distribution of electrons

For a nonthermal power law distribution of electrons $N(\gamma) = K_{\rm e}\gamma^{-p}$, we can obtain the total power per unit volume from

$$P_{\rm ic,tot} = \int_{\gamma_1}^{\gamma_2} P_{\rm ic} N(\gamma) d\gamma$$

This gives, for $\beta \simeq 1$,

$$\boxed{P_{\rm ic,tot} = \frac{4}{3}\sigma_{\rm T} c U_\gamma K_{\rm e}(3-p)^{-1}(\gamma_2^{3-p} - \gamma_1^{3-p}) \quad \text{nonthermal power-law electrons}} \tag{17}$$

- The spectrum resulting from single scattering events between a distribution of photons and a distribution of relativistic electrons predicts a power law spectrum with a spectral index

$$\alpha = 1/2\,(p-1)$$

- identical to the case of synchrotron emission. The power law spectrum is independent of the incident photon distribution.

- Example: Isotropic radio photons at 1 GHz IC scattered by electrons having g=10⁴ will be upscattered to the average frequency

$$\frac{\langle \nu \rangle}{\nu_0} = \frac{4}{3}\gamma^2$$

coresponding to X-ray radiation.

$$\langle \nu \rangle = 10^9 \text{ Hz } \frac{4}{3}(10^4)^2 \approx 1.3 \times 10^{17} \text{ Hz}$$

IC

Radiative case study:

Emission of SN 1006 produced by accelerated cosmic rays

E. G. Berezhko - L. T. Ksenofontov - H. J. Völk 2004

- Synchrotron emission flux as a function of frequency for the same two cases as in Fig. 2. Solid and dashed lines correspond to efficient and inefficient proton acceleration, respectively. The observed X-ray (in black color: Hamilton et al. 1986; in red color: Allen et al. 1999) and radio emissions (in black color: Reynolds 1996) are shown.

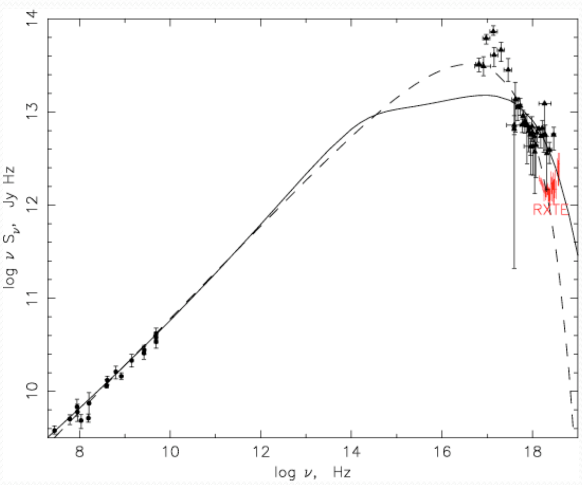

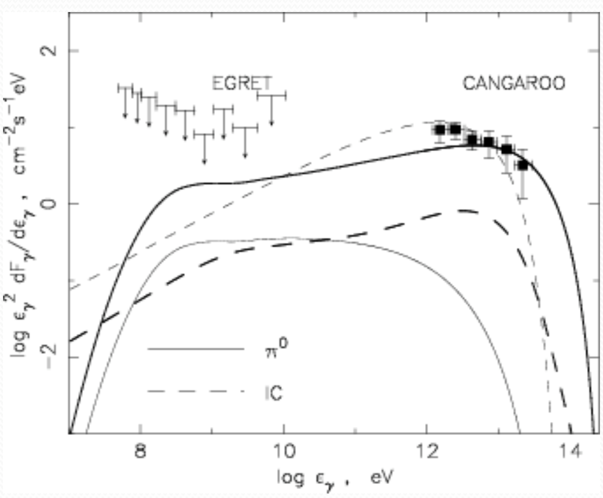

Synchrotron Self-Comptonisation

A particularly interesting case of inverse Compton scattering is that in which the seed photons are synchrotron photons emitted by the scattering electrons. In this case, the incident photon spectrum is the synchrotron power law spectrum, which can be written as

$$n(\varepsilon) = \frac{U_\gamma(\varepsilon_0)}{\varepsilon_0} \left(\frac{\varepsilon}{\varepsilon_0} \right)^{-(p-1)/2} \quad , \quad \varepsilon_{\min} \lesssim \varepsilon_{\max} \tag{24}$$

where ε_0 is some fiducial seed photon energy. The solution for the synchrotron self-Compton volume emissivity is

$$\boxed{j_{\nu_1}^{\mathrm{ssc}} = f(p) \sigma_{\mathrm{T}} c K_{\mathrm{e}} U_{\gamma \nu_0} \ln \left(\frac{\varepsilon_{\max}}{\varepsilon_{\min}} \right) \left(\frac{\nu_1}{\nu_0} \right)^{-(p-1)/2}} \tag{25}$$

A case study: Extragalactic

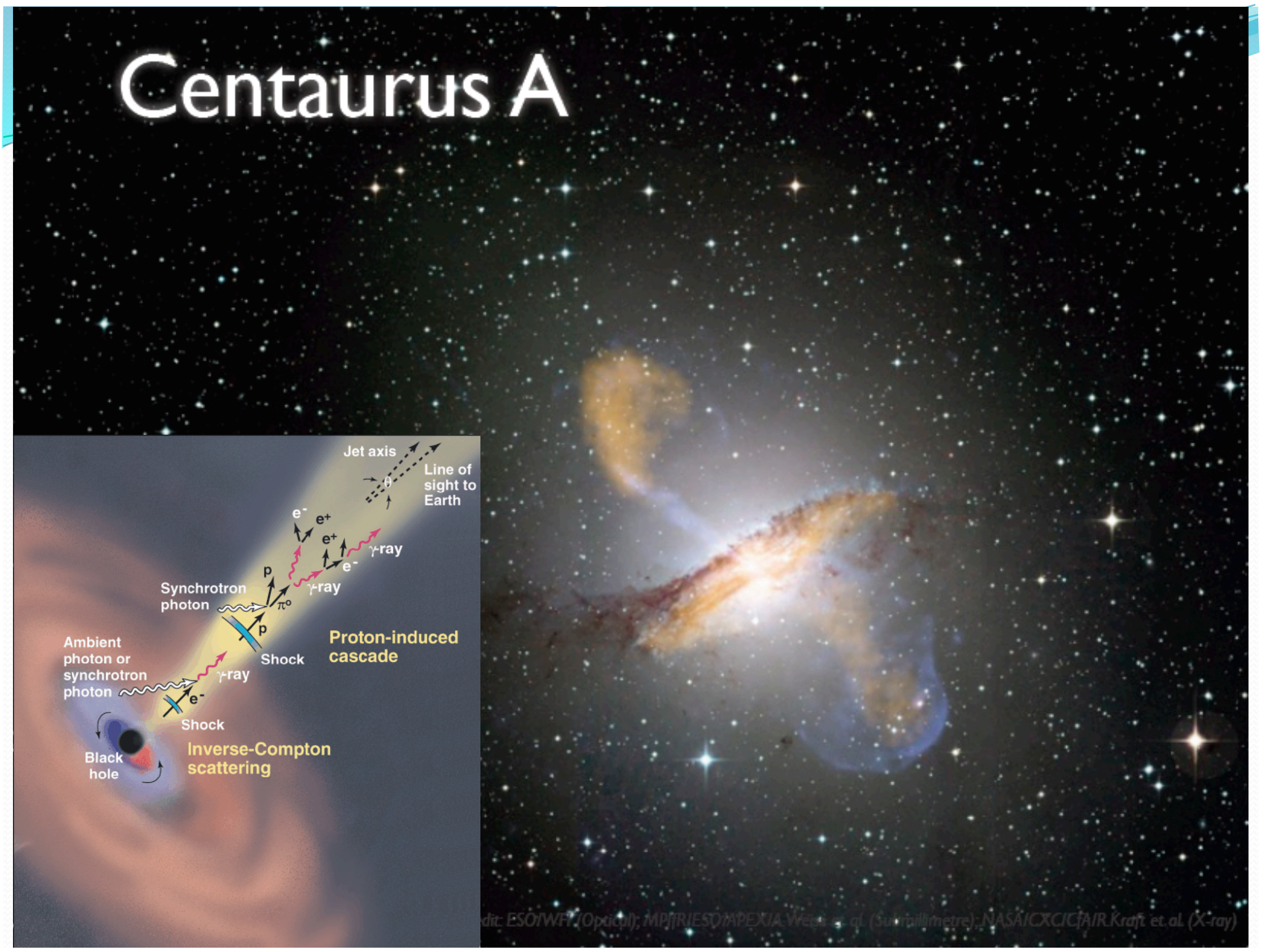

Multi-wavelength coverage of Cen A

- It's closeness can create problems, but Cen A provides us with a "front seat" in the AGN theater.
- We can investigate this AGN in so much detail, that it can well be, that Centaurus A will become the"Rosetta Stone"of AGN science

Cen A: FR I radio galaxy, non-blazar

- **distance ~ 3.4 Mpc**
- **central BH mass MBH ~ 108 MO**
- **under-luminous Lbol ~1043 erg/s**
- **jet velocity ~ 0.5c**
- **jet inclination (VLBI) > 50°, modest beaming**

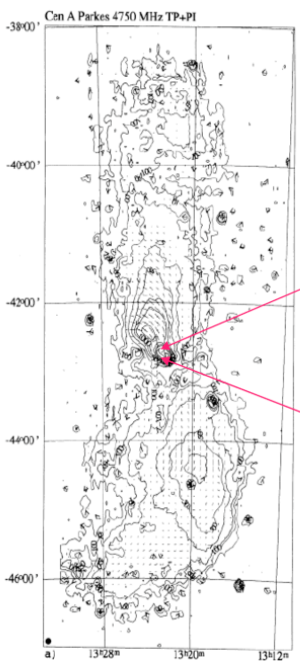

radio
5°x 9°

Dimensions

optical
12' x 8'

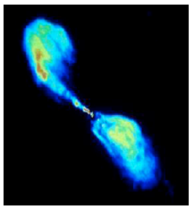

inner radio lobes
8' x 8'

all three pictures are same scale

X-ray
15' x 8'

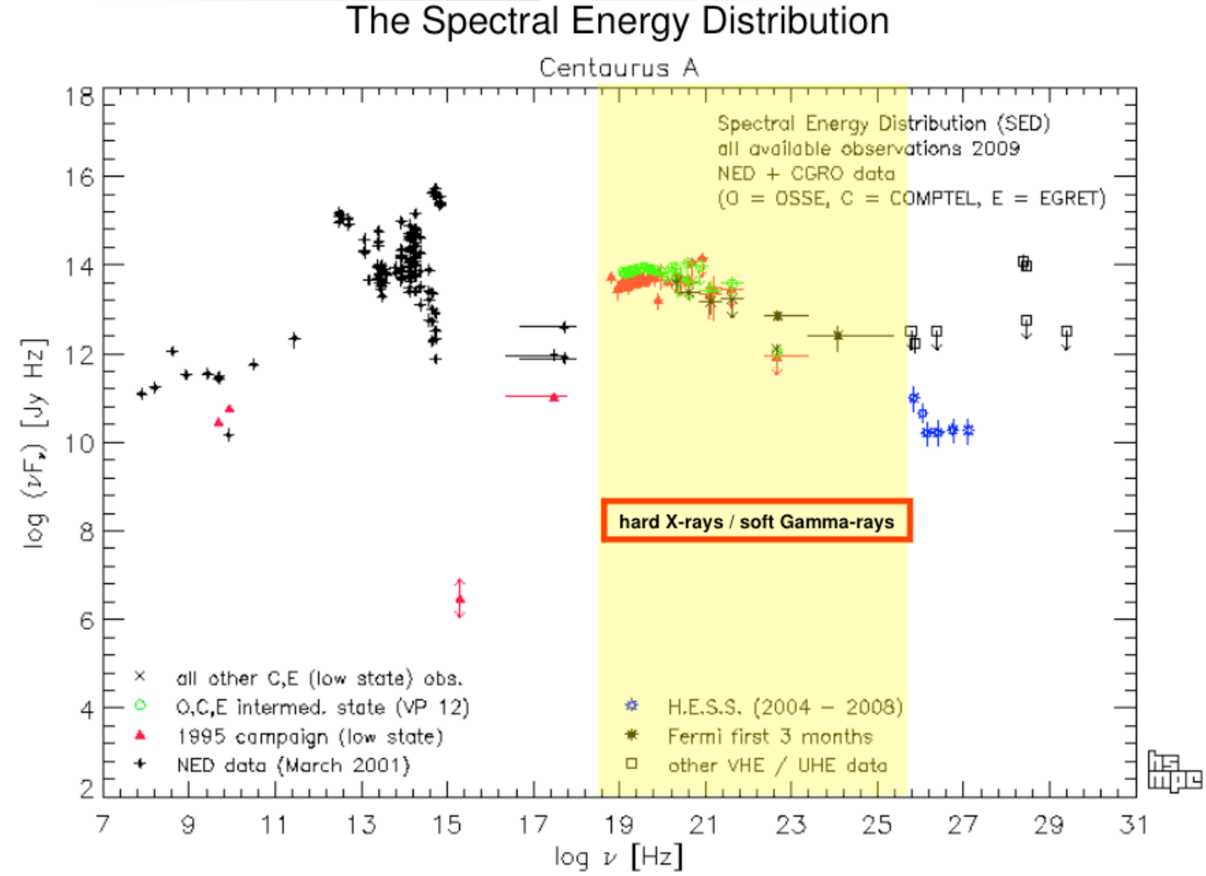

Steinle, MPE

Leptonic models of the inner jet

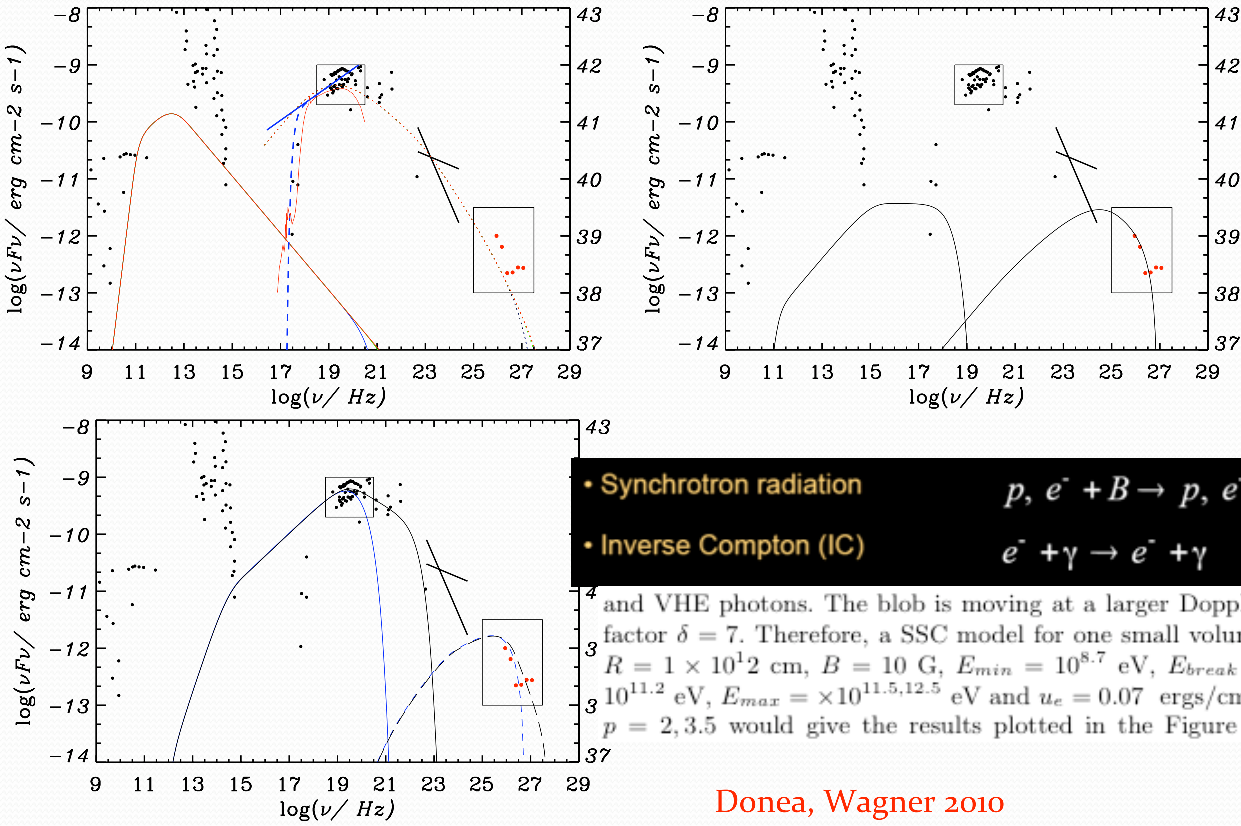

- Synchrotron radiation $p, e^- + B \rightarrow p, e^- + \gamma$
- Inverse Compton (IC) $e^- + \gamma \rightarrow e^- + \gamma$

and VHE photons. The blob is moving at a larger Doppler factor $\delta = 7$. Therefore, a SSC model for one small volume $R = 1 \times 10^12$ cm, $B = 10$ G, $E_{min} = 10^{8.7}$ eV, $E_{break} = 10^{11.2}$ eV, $E_{max} = \times 10^{11.5,12.5}$ eV and $u_e = 0.07$ ergs/cm^3, $p = 2, 3.5$ would give the results plotted in the Figure 4,

Donea, Wagner 2010

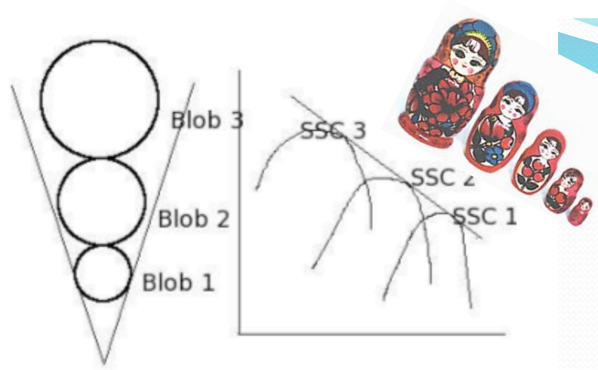

Figure 5. The Russian doll model for the gamma-ray SED in Cen A. The curve labeled SSC 1 corresponds to the e ·itting blob 1.

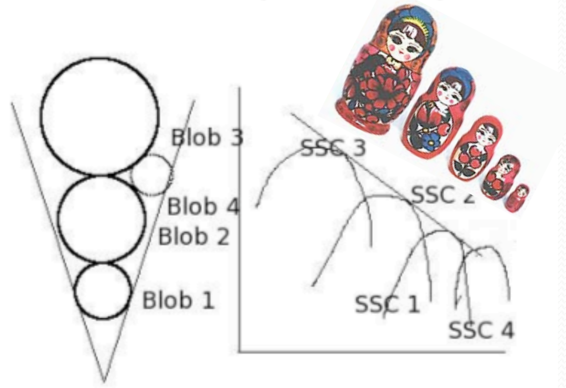

Figure 6. The Russian doll model for the gamma-ray SED in Cen A

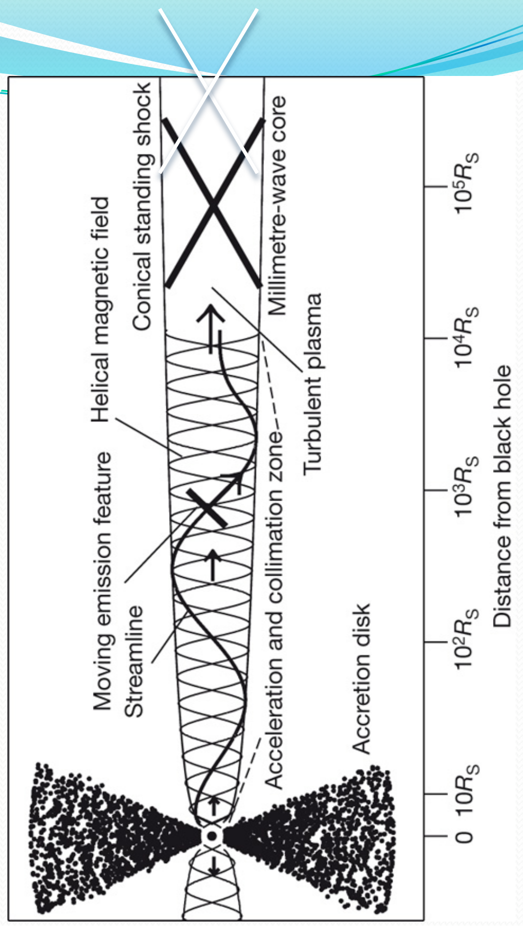

Proton-Proton Collisions

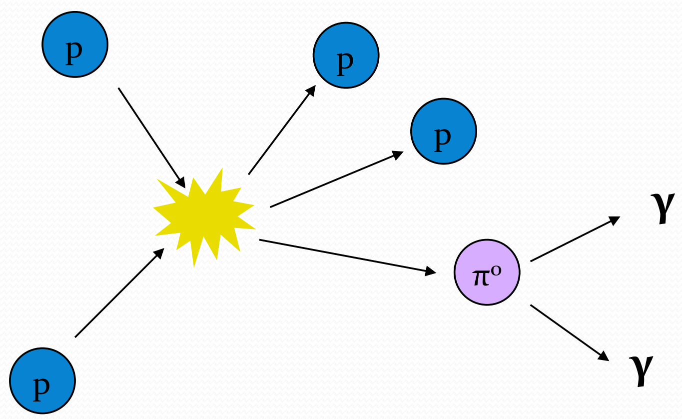

Decay of π^0

- hadronic (p-p) collisions of CRs with the gas nuclei.
- The π^0 meson has a slightly smaller mass of 135.0 MeV/c^2 and a much shorter mean lifetime of 8.4×10^{-17} s. This pion decays in a electromagnetic force process. The main decay mode, with probability 0.98798, is into two photons:

  $\pi^0 \rightarrow 2\gamma$

  Peak of SED: 67 MeV
- Its second most common decay mode, with probability 0.01198, is the so-called "Dalitz" decay into a photon and an electron-positron pair:

  $\pi^0 \rightarrow \gamma + e- + e+$

To calculate the π^0-decay γ-ray spectrum we adopt an empirical formula for the π^0 production spectrum developed by Stephens & Badhwar (1981), which allows us to use an arbitrary incident proton spectrum to calculate the π^0 production rate. The stellar parameters and calculated π^0-decay

Models of the galactic gamma-ray Background

Cosmic-ray propagation and interactions in the Galaxy
Andrew W. Strong , Igor V. Moskalenko, Vladimir S. Ptuskin 2007

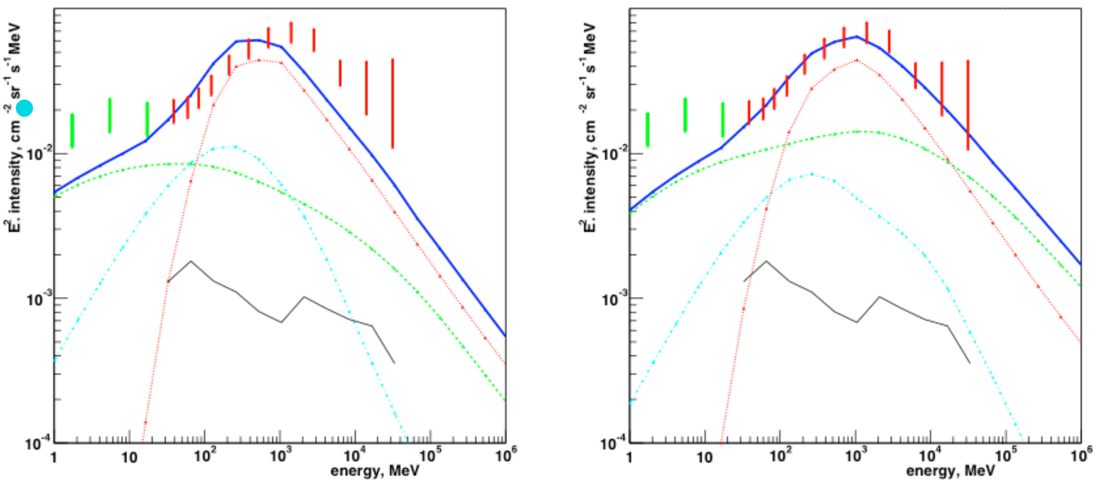

Figure 14: γ-ray spectrum of inner Galaxy ($330° < l < 30°, |b| < 5°$) for model based on the directly-observed CR spectra and modified spectra shown in Fig. 13. Red bars: EGRET data, including points above 10 GeV, see (151). Green bars: COMPTEL. Light blue line: bremsstrahlung, green line: inverse Compton scattering, red line: π^0-decay, black line: extragalactic background, dark blue line: total. This is an update of the spectra shown in (113).

Study case:

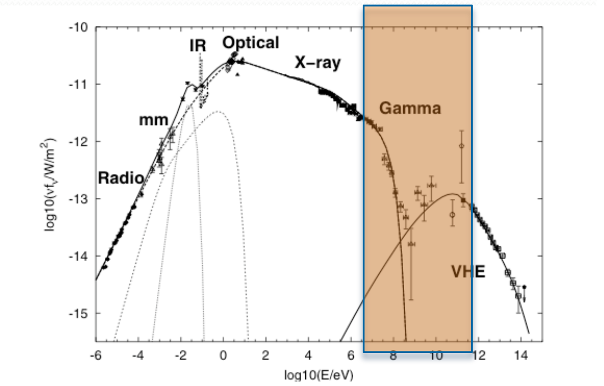

Figure 11: Broad-band SED of the Crab Nebula. The termination shock of the pulsar wind is an extreme accelerator boosting the energy of electrons to 10^{15} eV and beyond. In the framework of the synchrotron/inverse Compton emission model, it possible to explain the entire energy range from radio wavelengths to ultra-high energy gamma-rays. While the synchrotron radiation of $\geq 10^{14}$ eV electrons extends to the multi-MeV region, the inverse Compton scattering of the same electrons results in the ultra-high energy gamma-radiation detected by the HEGRA IACT system up to 50 TeV and beyond (see for details [71]).

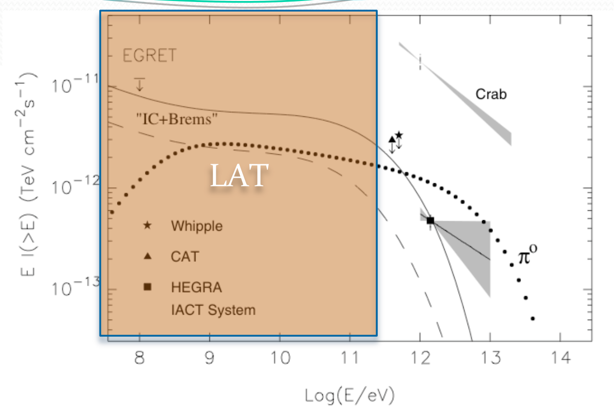

Figure 6: Gamma-rays from Cas A. The shaded area shows the 1σ error range for the fluxes measured by the HEGRA CT-system [19]. Also indicated are the flux upper limits set by EGRET, Whipple and CAT telescopes. Model predictions are presented by solid, dashed and dotted curves. The dotted curve represents the fluxes for π^0-decay decay γ-rays calculated for relativistic protons with power-law index $\Gamma = 2.15$ (identical to the spectral index of radio emitting electrons), exponential cutoff at $E_0 = 200$ TeV and total energy 2×10^{49} erg. The density in the shell is assumed $n = 15$ cm^{-3}. The solid and dashed lines correspond to the γ-ray fluxes produced by electrons calculated in the framework of a 3-zone model for 2 set of basic parameters discussed in Ref. [57].

The source is bright inX-rays, a noticeable fraction of which has nonthermal (synchrotron) origin

Study case:
A connection between star formation activity and cosmic rays in the starburst galaxy M82

The VERITAS Collaboration

Nature advance online publication 1 November 2009

Gamma-ray flux compared with a theoretical prediction.

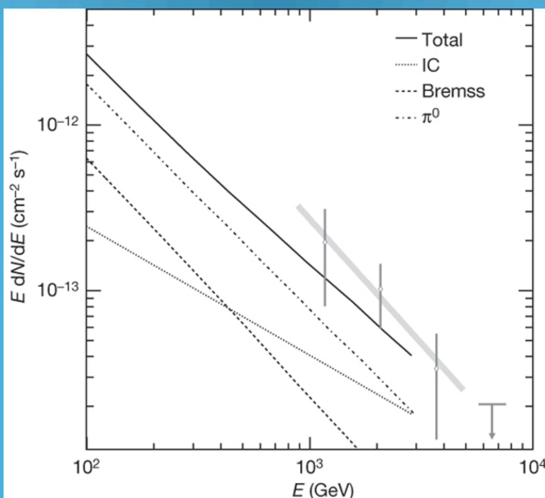

VA Acciari *et al.* *Nature* **000**, 1-3 (2009) doi:10.1038/nature08557

nature

More gamma ray emitters:

Pulsars are rapidly rotating, highly magnetized neutrons stars, born in supernova explosions of massive stars.

Typically, $M \sim 1.4\ M_{sun}$ and $R \sim 10$ km

A dense plasma is co-rotating with the star. The magnetosphere extends to the "light cylinder", where the rotation reaches the speed of light.

Emission (radio, optical, X-ray ...) can be produced in beams around the pulsar, which acts like a cosmic light-house.

~ 1900 pulsars known today. Vast majority in radio!

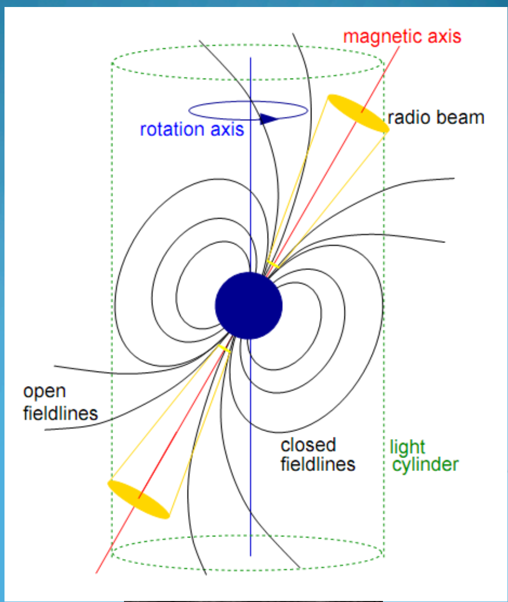

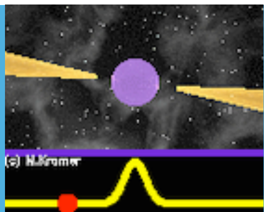

Protheroe, Donea, & Reimer 2003
Reimer, Protheroe, & Donea 2004

SPB Model Results for M87

- Input spectra from average SEDs
- Non-simultaneous data
- HE flux contributors:
  - p synchrotron (dashed)
  - $\mu^{\pm}$ synchrotron (dashed triple-dot)
  - π^{o} cascade (dotted)
  - $\pi^{\pm}$ cascade (dashed-dotted)

HBL model

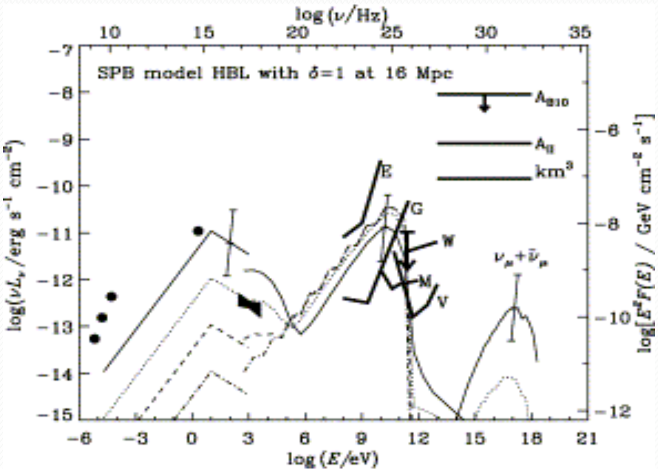

LBL model

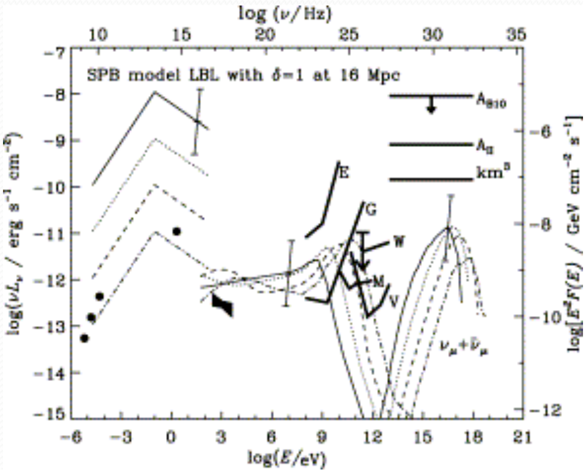

Time variability and multiwavelength campaigns for correlations

Models of the Extragalactic gamma-ray Background

- a sub-class of AGN, namely blazars, are strong gamma-ray emitters